CHARACTERIZATION STANDARD OF CMUT DEVICES BASED ON ELECTRICAL IMPEDANCE MEASUREMENTS

Franck TESTON[1], Cyril Meynier[1,2], Edgard Jeanne[3,4], Nicolas Felix[2] and Dominique Certon[1]
[1] - Université François Rabelais; LUSSI/CNRS FRE2448, 10 Bld Tonnellé BP3223 ~ 37032 Tours cedex
[2] - Vermon SA, Avenue du Général Renault ~ 37000 Tours
[3] - Université François Rabelais; LMP, 16 rue Pierre et Marie Curie BP 7155 ~ 37000 Tours
[4] – ST Microelectronics, 16 rue Pierre et Marie Curie BP 7155 ~ 37071 Tours Cedex 2
franck.teston@univ-tours.fr

***Abstract*— A procedure for a electrical impedance characterization standard in air of CMUTs was reported. The electromechanical coupling factor was calculated by the low and high frequency capacity and the resonance and antiresonance frequencies measurements. The cMUT will be able to analyze and compared in terms of effective spring and mass with 1-D model. The 1D model described the general behavior of the CMUT quite well, as long as first resonance/antiresonance mode and tensions below collapse were concerned.**

Keywords-component: Micromachined capacitive transducers; finite difference model, electrical impedance characterization.

I. INTRODUCTION

Capacitive micromachined transducers become now popular devices to design linear and annular arrays for standard or high frequency ultrasound imaging. Even if all cMUT work on the same physical principle, several manufacturing technologies exist for such devices, leading thus to great diversification in terms of final performances. The main degrees of freedom are the choices of the membrane, geometries, layout and patterning. When a new process is proposed, benchmarking with former technology is mandatory but difficult since the qualification parameters of the cMUT are mainly based on the electro-acoustic response of a transducer array that is greatly dependent on the electronic instrumentation used to drive the array element. So, there is a real need today to define simple intrinsic characteristics, such as the ones used in piezoelectricity domain, allowing to compare technologies between each others.

Capacitive transducers have been firstly described in the most way as mass spring items. Then, a large effort of 2D and 3D simulations is being done together with optical mapping of displacements, this helps to obtain detailed understanding of c-MUT functioning. However, in a fabrication process of complete array transducers, simple means of functional characterization will be needed and there the use of electrical measurements can be an easy and valuable tool provided it is supported by the adequate model. Recently, Lohfink [1] and Yaralioglu [2] demonstrate the interest of such 1-D model to simulate cMUT devices. The validity domain of such approach is defined thanks to comparison with finite element models and the key 1-D parameters are described. The main ones are the electromechanical coupling coefficient together with the mass, surface, stiffness and damping of the equivalent piston transducer from which mechanical impedance can be derived. Radiation impedance is of great importance when measuring loaded elements. Electrical parameters are the active and parasitic capacitance.

This paper describes the issues of a characterization protocol based on electrical impedance measurement. For the evaluation of the electro-mechanical coupling factor, two approaches are compared, one based on capacitance determination, the other on resonance and antiresonance peaks analysis. They are also compared to the electromechanical coupling factor and the electrical impedance theoretical results with 1D model and key parameters.

Finally, the characterization method will be illustrated on real measurements obtained on array elements with different shapes, layered structure membranes and different kinds of silicone nitride.

II. CMUT FABRICATION

For process [3], 500µm thick n-type <100> Si wafers were used. The first step was the growth of a field oxide 1.2 µm thanks to a wet thermal oxidation. Then a 0.45 µm thick polysilicon layer was deposited by LPCVD (Low Pressure Chemical Vapour Deposition) and was $POCl_3$ doped. This layer is the bottom electrode. A thin sacrificial layer of silicon oxide was done by PECVD (Plasma Enhanced CVD) and determined by its thickness the gap height. Then the sacrificial oxide layer was patterned too in order to define the cell geometries. The bottom electrode was also patterned in order to reduce the parasitic capacitance. The membrane material was a silicon nitride (SiN) realized by LPCVD, with a thickness of 0.45µm.

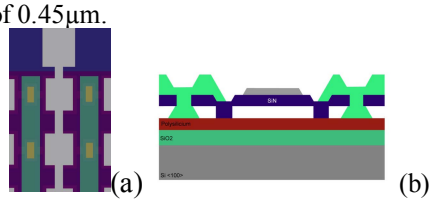

Figure 1. (a) Top view after top electrode patterning; (b) cross-section view

Several SiN layers were processed exhibiting different stochiometry and then internal stresses. A dry etching step was necessary for opening of SiN layer to access sacrificial layer. The final application being in immersion, the cavities had to be sealed. This was realized by depositing a 0.8 µm thick USG (Undoped SG) which was patterned over the SiN holes. A 0.35µm thick layer of Aluminum was sputtered and patterned

in order to create the top electrode of the cMUT. The final structure obtained is illustrated in the Figure 1.

Two square-shaped membrane types were chosen for cMUTs cell, a 20*20 and 25*25 μm^2, with different inter-membrane spacing. All tested configurations were array elements with the same inter-element spacing, pitch and transverse aperture dedicated to the same targeted application. Different silicon nitride membrane materials were manufactured and investigated : mid-stress nitrides ($\sigma \cong 200MPa$) were used in "A", "B" and "C" wafers, and very-low stress nitrides ($\sigma <$ 150MPa) were used in "D" and "E". All were lower in stress than standard stochiometric Si_3N_4 used in semiconductor industry.

Nitride	Gap (nm)	Spacing	20x20		25x25	
			Ref.	Nb cells	Ref.	Nb cells
Mid-Stress	200	Wide	A1	264	-	-
Mid-Stress	200	Dense	B1	330	B2	285
Mid-Stress	200	Wide	C1	264	C2	228
Low-Stress	200	Wide	D1	264	D2	228
Low-Stress	100	Wide	E1	264	-	-

TABLE I. SUMMARY OF CMUT ASSEMBLIES
A AND B ARE FROM THE SAME WAFER, OTHERS ARE FROM DISTINCT WAFERS

III. ELECTRICAL IMPEDANCE PROTOCOL

Input electrical impedance in air was measured as a function of frequency. Measurements were performed using two techniques : an auto-balanced bridge analyzer (HP4294A) and popular reflectometry analyzer (HP8753ET). In this case, a standard calibration (short and open circuit, resistance and capacitance load) was operated. CMUTs were polarized using classical DC-bias decoupling circuit.

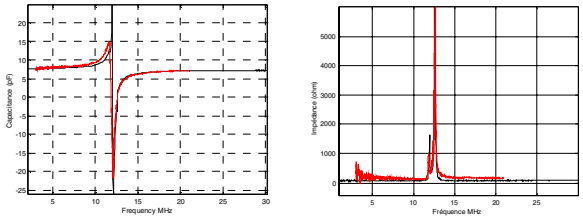

Figure 2. Comparison of D1 CMUT capacity and real part of impedance versus frequency (red : HP8753ET and black : HP4294A).

Figures 2 show the real part of impedance and the capacitance. A good agreement can be observed for the resonance frequency and the low and high frequency capacitances. But auto-balanced bridge allows to obtain a better signal to noise ratio at low frequency and a good measurement in a wider range. The impedance measurement accuracy at four-terminal pair port of the Agilent 4294A's was better than 3 % in the 1-20 MHz range for 1 to 10 pF capacitance, whereas with the HP 8753ET was larger than 10%. This demonstrated that the accurate choice of instrument for impedance analysis was mandatory for sharp cMUT electrical impedance measurement.

IV. 1-D MODEL AND KEY PARAMETERS

The usual formulation of 1D model, well described in references [1, 2], was reduced to four parameters: electrode surface S, mass m of the movable part, spring stiffness k and effective gap z_0, this variant allow prediction of static deflection Z(Vdc), collapse and snapback voltage, and change of resonance frequency due to electrostatic softening. Here, two extra parameters were added : a linear mechanical damping term, σ, and a parallel parasitic capacitance, $\mathbf{C_p}$. This extended the use of the model to prediction of impedance curves that can be compared directly to experimental results.

In a behaviorist approach, parameters (k, m, σ) were calculated from the main experimental results (V_c, f_0, Q) using main equations of the model :

$$k = \frac{27}{8}\varepsilon_0 S \frac{V_c^2}{h_{eq}^3} \quad (1)$$

where $h_{eq} = h_{gap} + \frac{h_m}{\varepsilon_r}$

$$m = \frac{k}{2\pi f_0^2} \quad (2)$$

Alternatively, in a predictive approach, they were computed from geometrical dimensions and material properties obtained by process knowledge and test structures. For refinement a more accurate model such as Finite Difference model [4] or FEA tool can be used for accurate modeling, but for such purpose 1-D model is sufficient. Below is displayed the good agreement between experimental results and 1D behaviorist simulation for a D1 cMUT element :

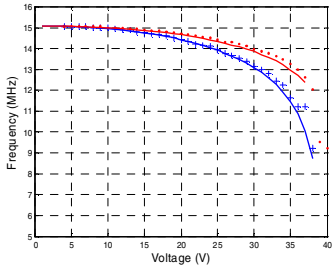

Figure 3. Comparison between experimental frequencies (points and crosses) and 1-D model (lines)

The experimental resonance and antiresonance frequencies (f_r and f_a) correspond, respectively, to the real part of admittance and impedance peak for each polarization voltage. They were compared with the model's prediction, where resonance frequencies were shifted by the spring softening effect:

$$\tilde{\omega}_r(V_{stat}) = \sqrt{\frac{\tilde{k}(V_{stat})}{m}} = \sqrt{\frac{k - \frac{S\varepsilon_0 V_{stat}^2}{z_{stat}^3}}{m}} \quad (3)$$

The theoretical antiresonance frequency also droped with polarization, due to the effect of parasitic capacitance. A very good fit could be observed between measurements and theoretical prediction.

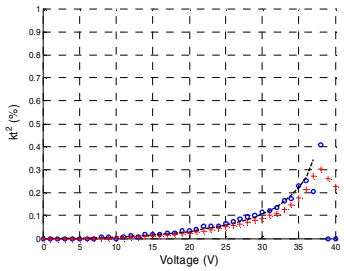

Figure 4. Electromechanical coupling factor
dashed line is model; circles and crosses are respectively frequency and capacitance-defined experimental results.

There were two ways to extract kt^2 from measurement results: one defines it according to f_r and f_a, while the other uses LF and HF capacitances [4]. Theoretically, they are equivalent provided there is only one mode. If not, the capacitance-based definition gives a value that encompass all the modes. On the figure 4, the model's value was compared with experimental results using both definitions.

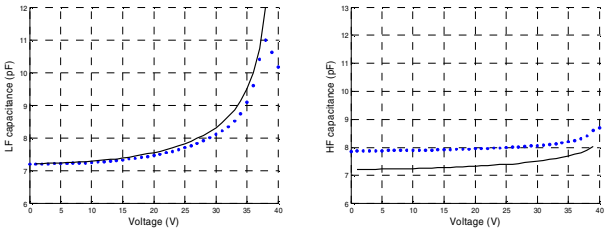

Figure 5. Low and high frequency capacitance compared to the 1-D model.

LF capacitance was well fitted to the model, as shown on the figure 5. There was an offset in measured HF capacitance, even without bias, due to the non-linearity of the dielectric (ε_r varies with frequency).

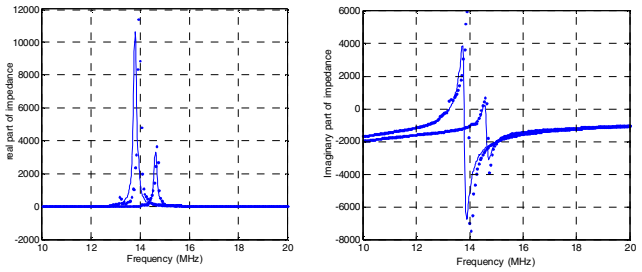

Figure 6. Real and imaginary part of electrical impedance. (1-D modeled line and measured points are shown for different bias voltage 20 and 30 Volts)

With mechanical damping taken into account as a solid friction term fitted to the measured quality factor, impedance curves of the 1D model can be determined. Figures 6 show the fit between experimental and theoretical data of the real and imaginary part of cMUT impedance for V_{dc} values of 20 and 30 volts. A good agreement can be observed in the two cases.

V. RESULTS AND COMPARISON

This section presents the experimental results on cMUT manufactured for square shape cMUT and discussion with key parameters obtained by fitting 1D model.

A. Influence of inter-membrane spacing

A1 and B1, in addition to membrane spacing, have slight differences in design, that may explain their different stiffness. Dispersion in nitride thickness may also be involved.

Very high values of kt^2 (up to 50%) were obtained for 20x20 designs, as shown on Figure 7. 25x25 don't reach such high kt^2, due to the difference between boundary conditions inducing cell behavior and static deflection sensitivity.

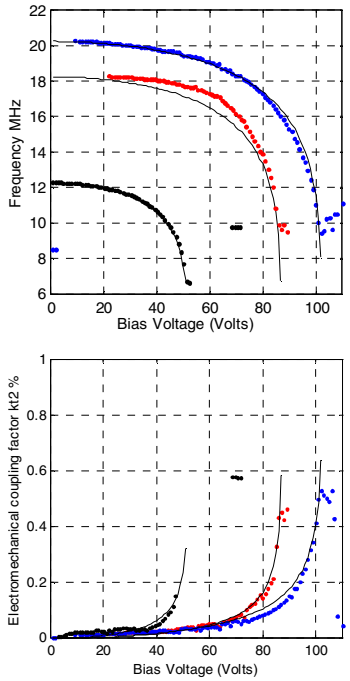

Figure 7. Resonance frequency and electromechanical coupling coefficient versus bias voltage for square configurations (A1 blue, B1 red and B2 black).

B. Influence of silicon nitride material

Firstly, tested configurations were those of the A and C wafers. The C configuration was chosen because the mid stress SiN used for this run is very similar to A one. When comparing each configuration for the two processes, Figure 8 show that resonance frequencies and collapse voltages values were smaller for the C wafer. Main reasons were the thickness membrane diminution (measured to around 50 nm using electronic microscopy) due to unperfect selectivity of the HF etching and initial static deflexion of the membrane induced by the latest process steps. But, the initial deflexion changed only collapse voltage without modifying resonance frequencies.

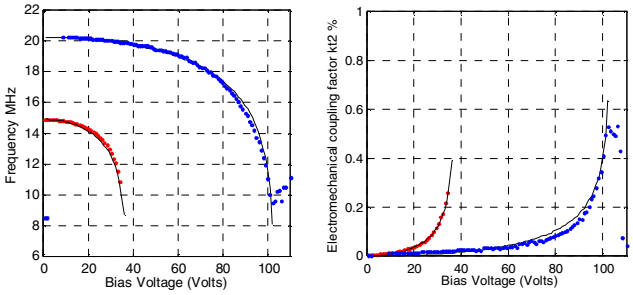

Figure 8. Resonance frequency and electromechanical coupling coefficient versus bias voltage for configurations : A1 blue and C1 red.

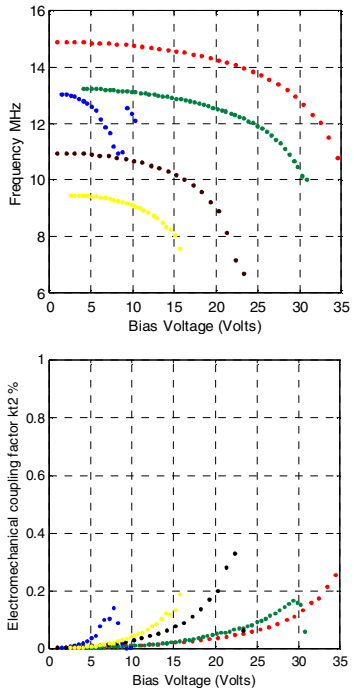

Figure 9. Resonance frequency and electromechanical coupling coefficient versus bias voltage for square cMUT : C1 red and C2 black ; D1 green and D2 yellow ; E1 blue.

Figures 9 show the resonance frequency and electromechanical coupling factor. Secondly, the comparison between wafer D1 and wafer E1 shows, as expected, that the resonance frequency does not change with the gap thickness, only collapse voltage. Similar mass values were obtained and the ratio between the stiffness was k_{D1}/k_{E1} = 1.03. This confirms that membranes were well reproduced between D1 and E1. The collapse voltage was determined by electrode surface, stiffness, and initial equivalent gap. Thus, from equation (1), a good agreement can be obtained between the ratio $\left(\frac{h_{gap}^{D1}}{h_{gap}^{E1}}\right)^3$ and $\left(\frac{V_{D1}}{V_{E1}}\right)^2$.

More variations between mid stress (C1) and low stress SiN were consistent since the sample D1 displayed the lowest resonance frequency and collapse voltage.

Some data can be extracted from the comparisons between the 20x20 (D1) and 25x25 (D2) membranes. The ratio between their fundamental frequencies was f_{D1}/f_{D2} = 1.38, whereas we expected 1.25 from theoretical value for a clamped plate was in the 1/L form [6]. However the 25x25 design was not an exact scale-up of the 20x20 design. If we assumed the ratio of masses was 0.64 (geometrical), a reasonable assumption since both samples were from the same wafer, we can deduce the ratio between the stiffness: k_{D1}/k_{D2} = 1.22. Samples C1 and C2 give almost the same results, since the ratio of their resonance frequencies was 1.36.

Figure 10 displays the variation of LF capacitance of a 20x20 sample (D1) during a polarization cycle up to 40 volts and back to zero. The two distinct curves (conventionnal and collapsed modes) were clearly observed, as well as the hysteresis between collapse and pull-out. The transitions were not vertical due to dispersion.

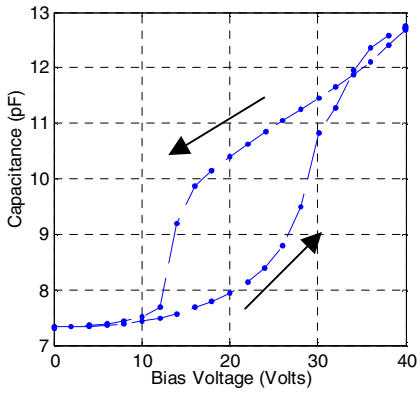

Figure 10. The capacitance of a cMUT element as a function of bias up to collapse voltage.

VI. CONCLUSION

A electrical impedance characterization procedure for cMUT has been presented. The fitting of the experimental input electromechanical coupling factors and the resonance frequencies versus bias voltage with a 1D model allows us to determine the important key parameters (mass and rigidity) for cMUT array element.

This simple 1D-model, when applied to a wafer that constitutive parameters (membrane stress, Young modulus, permittivity,…) were well known, fitting of typical curves such as k_t^2(Vdc) and f_r(Vdc) allowed an accurate determination of membrane and gap thicknesses for example. Therefore if this constitutive parameters were unknown, using different geometrical configurations (membrane dimensions and inter-element spacing) measurements, it was possible to extract constitutive parameters. This quick characterization procedure will be very useful for wafer to wafer and batch to batch comparison.

ACKNOWLEDGMENT

This work was performed through the research project MEMSORS labeled by the EUREKA's cluster program EURIMUS and funded by the French Ministry of Finances / Direction Générale des Entreprises (DGE).

REFERENCES

[1] A. Lohfink and P. Eccardt, "Linear and Non linear Equivalent Circuit Modeling of CMUTS", IEEE-UFFC, vol. 52, pp. 2163-2172, December 2005.

[2] G. Yaralioglu et al., "Finite-Element Analysis of Capacitive Micromachined Ultrasonic Transducer", IEEE-UFFC, vol. 52, pp. 2187-2198, December 2005.

[3] B Belgacem et al « Optimization of the fabrication of sealed capacitive transducers using surface micromachining », 14 299-304, J. Micromech. Microeng., 2004

[4] D. Certon, F. Teston, and F. Patat " A Finite Difference Model For cMUT Devices", Capacitive Micromachined Ultrasonic Transducers Special Issue in IEEE Transaction on Ultrasonics, Ferroelectrics and Frequency Control, vol.52, n°12, pp2199 - 2210, 2005.

[5] G. Yaralioglu et al., "Calculation and measurement of electromechanical coupling coefficient of capacitive micromachined ultrasonic transuders", IEEE-UFFC, vol. 50, pp. 449-456, 2003.

[6] M Géradin & D.Rixen, THEORIE DES VIBRATIONS," Applications à la dynamique des structures", Edition MASSON, Paris 1993.